EFFECT OF CATALYST CIRCULATION RATE ON THE BIFURCATION BEHAVIOR OF AN INDUSTRIAL FCC UNIT

A. E. Abasaeed

Non-linear Dynamics Group (NLDG), Chemical Engineering Department
King Saud University
P.O. Box 800, Riyadh 11421, Saudi Arabia

الخلاصة :

لقد تَـمَّـتْ دراسة تأثير معدل دورة العامل الحفاز (١٧,٧٢١ - ١٥٠,٦٣ كجم/ث) على التصرف التشعبي لوحدة تكسير حفزية صناعية للنظامين المفتوح والمغلق . أثبتت الدراسة وجود خمس مناطق ذات اختلافات نوعية في التصرف التشعبي . وبتحليل نتائج النظام المفتوح وُجد أنَّ تقليل معدل دورة العامل الحفاز يؤدى الى استقرار النقطة ذات الانتاج الأعلى لمادة الجازولين ، ولكن هذا يحتم زيادة درجة حرارة الهواء الداخل في وحدة التنشيط . أما بالنسبة لتحليل نتائج النظام المغلق فلقد أثبتت الدراسة أن استقرار النقطة ذات الانتاج الأعلى لمادة الجازولين يتطلب وجود قيم أعلى لمعامل جهاز التحكم التناسبي عند زيادة معدل دورة العامل الحفاز .

ABSTRACT

The effect of catalyst circulation rate (17.721–150.63 kg/s) on the bifurcation behavior of an industrial fluid catalytic cracking (FCC) unit is investigated for both the open loop as well as the closed loop systems. Five regions of qualitatively different bifurcation behavior are identified. For the open loop system it is found that decreasing the catalyst circulation rate stabilizes the point of maximum gasoline yield but higher values of air feed temperatures are required. The closed loop analysis shows that higher value of controller gains are required to stabilize the point of maximum gasoline yield as the catalyst circulation rate is increased.

A. E. Abasaeed

EFFECT OF CATALYST CIRCULATION RATE ON THE BIFURCATION BEHAVIOR OF AN INDUSTRIAL FCC UNIT

1. INTRODUCTION

The economics of petroleum refineries are greatly enhanced by efficient operation of their fluid catalytic cracking (FCC) units which convert heavy hydrocarbons into gasoline and lighter hydrocarbons. Previous studies revealed that the multiplicity of steady states phenomenon exists in these units and also that FCC units are usually operated at the middle unstable steady state in order to give high yield of the desired product [1–6]. The models developed by Elshishini and Elnashaie [4, 6] for industrial FCC units (conversion of gasoil to gasoline) were very successful in representing a number of these units and they confirmed the operation of the unit at the middle unstable saddle type steady state. The above models were recently extended by Elnashaie *et al.* [7] to include the dynamics of gasoil as well as gasoline.

The two-subunits (reactor and regenerator) of the FCC unit are coupled through catalyst circulation. Therefore, in this paper a detailed investigation of the effect of catalyst circulation rate (*CCR*) on the bifurcation behavior of an industrial FCC unit for the open loop system is conducted. The operating conditions that give maximum gasoline yield are identified and used to investigate the closed loop system when a feedback proportional controller is used.

2. THE MODEL

The model used here is similar to the previously developed model by Elnashaie *et al.* [7] The model uses the 2-phase theory for fluidization (a completely mixed dense phase where all reactions take place and a plug flow regime for the bubble phase). The hydrodynamic parameters are obtained from Kunii and Levenspiel [8]. A 3-lump kinetic model [9] together with data obtained from the plant for coke fraction and heavy cycle oil are used in developing the model. The model equations are briefly explained (for detailed development of the model see [4, 6, 7]) and presented in a normalized form as Equations (1)–(8).

The reactor dense phase dimensionless temperature is given by:

$$\frac{dY_{RD}}{d\tau} = B(Yv - Y_{RD}) + A_2(Yf - Yv) - Hv + HRCB + A_1(Y_{GD} - Y_{RD}) - HL_R \tag{1}$$

In the right hand side of Equation (1), the first 3 terms represent the amount of heat required to raise the temperature of the feed to the reactor dense phase temperature. The fourth term is the heat added due to reaction, the fifth term gives the heat exchange between regenerator and reactor, and the last term accounts for heat losses from the reactor.

The regenerator dense phase dimensionless temperature is given by:

$$\frac{dY_{GD}}{d\tau} = \xi_1\left\{BD(Y_{fa} - Y_{GD}) + \beta c(CB) + A_3(Y_{RD} - Y_{GD}) - HL_G\right\}. \tag{2}$$

The first term is heat added by air used to burn-off the coke, the second term represents heat added due to coke burning, third term gives the heat exchange between reactor and regenerator, whereas the last term is the heat losses from the regenerator.

The gasoil mass balance in the reactor is given by:

$$\frac{dX_{go}}{d\tau} = \xi_2\left(B\left\{X_{gof} - X_{go}\right\} - \psi_R\left[\alpha_1 \exp(-\gamma_1/Y_{RD}) + \alpha_3 \exp(-\gamma_3/Y_{RD})\right]X_{go}^2\right). \tag{3}$$

The first term gives the balance between gasoil entering with the feed and that leaving the reactor, and the last two terms are for gasoline and coke formation respectively.

The gasoline mass balance in the reactor is given by:

$$\frac{dX_{gd}}{d\tau} = \xi_3\left\{B(X_{gdf} - X_{gd}) - \psi_R\left[\alpha_2 X_{gd}\exp(-\gamma_2/Y_{RD}) - \alpha_1(X_{go})^2\exp(-\gamma_1/Y_{RD})\right]\right\}. \tag{4}$$

The balance between gasoline in the feed and that leaving the reactor is given by the first term. The second term represents gasoline depletion (to coke), and the third term gives gasoline formation.

The catalyst activity in the reactor is given by:

$$\frac{d\psi_R}{d\tau} = \xi_4(C_{RD}\{\psi_G - \psi_R\} - \psi_R . R_c). \tag{5}$$

The first term represents catalyst exchange between the regenerator and the reactor. The second term is for the loss of catalyst activity due to coke formation.

The catalyst activity in the regenerator is given by:

$$\frac{d\psi_G}{d\tau} = \xi_5\{CB - C_{GD}(\psi_G - \psi_R)\}. \tag{6}$$

The first term is for coke burning rate and the second term is for catalyst exchange between the regenerator and the reactor.

The air feed temperature is given by:

$$Y_{fa} = Y_{fso} + Kc(Y_{sp} - Y_{RD}). \tag{7}$$

It is clear from Equation (7) that $Kc = 0$ corresponds to the open loop case.

The catalyst circulation ratio, F_{CDS}, is defined by Equation (8).

$$F_{CDS} = \frac{CCR}{88.605} \tag{8}$$

In all the Equations (1–8), we define:

$$A_1 = \frac{Fc . C_{ps}}{A_{IR} . H_R . C_{pf}} \qquad A_2 = \frac{F_G . C_{pl}}{A_{IR} . H_R . C_{pf}} \qquad A_3 = \frac{Fc . C_{ps}}{A_{IR} . H_G . C_{pa}}$$

$$\alpha_1 = K_{10} . \varepsilon . C_{alf} \qquad \alpha_2 = K_{20} . \varepsilon \qquad \alpha_3 = K_{30} . \varepsilon . C_{alf}$$

$$\beta_c = \frac{Cm.(-\Delta H_c)}{T_{RF} . C_{pa} . \rho_a} \qquad B = \frac{G_{IR} + G_{CR}\,1 - \exp(-a_R H_R)}{A_{IR} . H_R} \qquad BD = \frac{G_{IG} + G_{CG}\,1 - \exp(-a_G H_G)}{A_{IG} . H_G}$$

$$\xi_0 = \frac{W_R . C_{ps}}{(A_{IR} . H_R . C_{pf} . \rho_f)} \qquad \xi_1 = \frac{\xi_o . (A_{IG} . H_G . C_{pa} . \rho_a)}{W_G . C_{ps}} \qquad \xi_2 = \frac{\xi_o . (A_{IG} . H_G . C_{pa} . \rho_a)}{W_G . C_{ps}}$$

$$\xi_3 = \frac{\xi_o \cdot (A_{IG} \cdot H_G \cdot C_{pa} \cdot \rho_a)}{W_G \cdot C_{ps}} \qquad \xi_4 = \frac{\xi_o \cdot (A_{IR} \cdot H_R \cdot C_{a/f})}{W_R \cdot Cm} \qquad \xi_5 = \frac{\xi_o \cdot (A_{IG} \cdot H_G)}{W_G}$$

$$\tau = \frac{t}{\xi_o} \qquad C_{RD} = \frac{Fc \cdot Cm}{A_{IR} \cdot H_R \cdot C_{alf}} \qquad C_{GD} = \frac{Fc}{A_{IG} \cdot H_G}$$

$$a_R = \frac{Q_R \cdot A_{CR}}{G_{CR}} \qquad a_G = \frac{Q_G \cdot A_{CG}}{G_{CG}}$$

3. RESULTS AND DISCUSSION

The analysis presented in this paper is for an industrial fluid catalytic cracking unit. The industrial unit is operated at a catalyst circulation rate, CCR = 88.605 kg/s and the dimensionless air feed temperature (Y_{fa}) is 0.872. The detailed design and operating conditions of this important unit were given in Table 1. These operating

Table 1. Plant Data for Unit 1.

Fresh feed	16.782 kg/s
Recycled HCO	2.108 kg/s
Combined feed ratio (CFR)	1.1256
Air flow rate	10.670 kg/s
Catalyst circulation rate	88.605 kg/s
Combined feed temperature	527 K
Air feed temperature	436 K
Y_{fa}	0.872
Hydrogen in coke (wt%)	4.17
HCO/(HCO + CSO + LCO)	0.286
Coke/(coke + gases)	0.221
$CO_2/(CO_2 + CO)$	0.75 (m^3/m^3)
$(-H_c)$	31235.6 kJ/kg
Regenerator dimensions	5.334m ID × 14.859m
Reactor dimensions	3.048m ID × 12.760m
Catalyst retention in reactor	17.5 metric tons
Catalyst retention in regenerator	50 metric tons
API of raw oil feed	28.7
Reactor pressure	225.4938 kPa
Regenerator pressure	254.8708 kPa
Average particle size	0.00072 m
Pore volume of catalyst	0.00031 m^3/kg
Apparent bulk density	800 kg/m^3
Catalyst surface area	215 m^2/g

conditions correspond to a middle (saddle-type) unstable steady state as shown by Elshishini and Elnashaie [4]. This investigation focuses on the effect of catalyst circulation rate on the bifurcation behavior of this industrially important unit. The investigation covers a wide range of *CCR* (17.721–150.63 kg/s) corresponding to F_{CDS} range of (0.2 to 1.7). In the following analysis, AUTO86 developed by Doedel and Kernevez [10] is used to construct the bifurcation diagrams.

3.1. Open-Loop Bifurcation Behavior

Figure 1 shows a two-parameter continuation diagram for the catalyst circulation ratio, F_{CDS}, (defined by Equation (8)) against the dimensionless air feed temperature, Y_{fa}. The two-parameter continuation diagrams are concise representations of the loci of static limit points (SLP) and Hopf bifurcation (HB) points. The solid horizontal lines in the figure separates regions of qualitatively different bifurcation behavior. The dashed curves in the figure represent the loci of static limit points whereas the solid curve shows the loci of the Hopf bifurcation point. Actually, two solid curves of the loci of Hopf bifurcation points are present. For clarity reasons the second solid curve (loci of a second HB point) is not shown on the figure because this loci moves very closely along the side (slightly to the left) of the loci of the static limit point represented by the dashed curve extending beyond $F_{CDS} > 1.5$. This point becomes more clear when Figure 2 is discussed. It is clear from Figure 1 that the solid horizontal lines separates the diagram into 5 distinct regions.

3.1.1. First Region, R1 ($F_{CDS} > 1.502964$)

This is the region for which $F_{CDS} > 1.502964$ (corresponding to the tip of the cusp of the limit points loci). In this region one static limit point and one Hopf bifurcation point (the degenerate HB point is not shown in the figure) exist. The open-loop bifurcation diagram for $F_{CDS} = 1.7$ is shown in Figures 2(*a*), (*b*) which show the

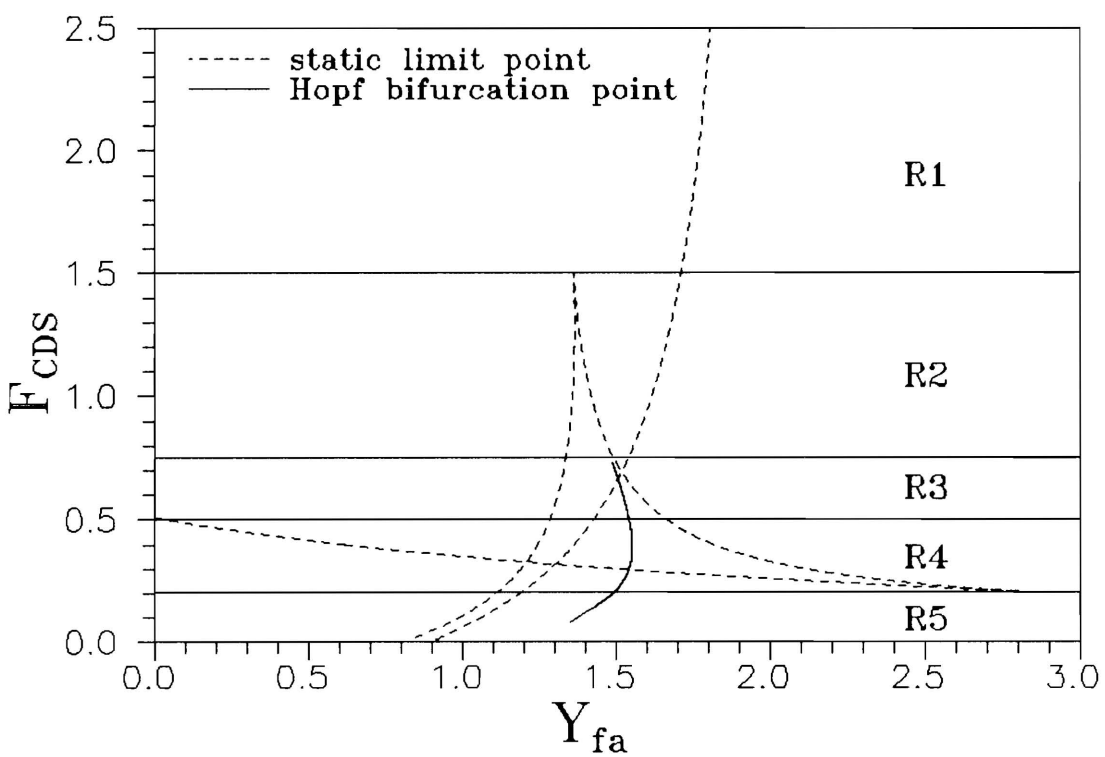

Figure 1. Two-Parameter Continuation Diagram for the Catalyst Circulation Ratio, F_{CDS}, Against the Air Feed Temperature, Y_{fa}. Solid horizontal lines separates regions of different bifurcation behavior.

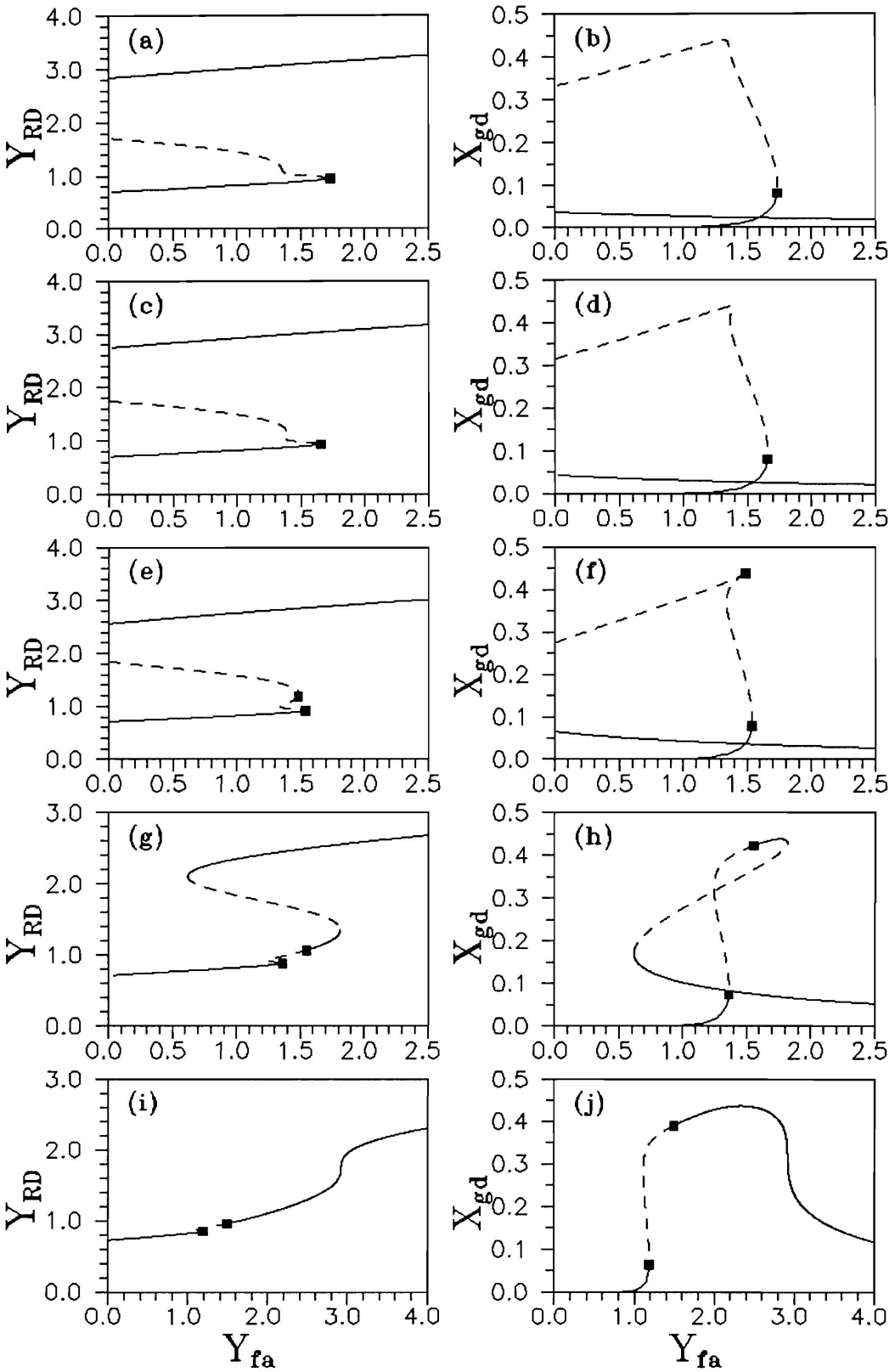

Figure 2. Bifurcation Diagrams for the Open Loop System for Reactor Dense Phase Temperature, Y_{RD}, and Gasoline Yield, X_{gd}, Against the Air Feed Temperature, Y_{fa}. (a, b for Catalyst Circulation Ratio, F_{CDS} = 1.7); (c, d for F_{CDS} = 1.2); (e, f for F_{CDS} = 0.75); (g, h for F_{CDS} = 0.4); and (i, j for F_{CDS} = 0.2).

bifurcation behavior for the reactor dense phase temperature, Y_{RD} and dense phase gasoline yield, X_{gd} respectively against the dimensionless air feed temperature. The solid lines in these figures represent stable static steady state branches whereas the dashed lines represent unstable static branches. The Hopf bifurcation point is represented by the symbol (■). Note that the degenerate Hopf bifurcation point (at $Y_{fa} = 1.733355$) is very close to the static limit point (at $Y_{fa} = 1.736741$). Figure 2(*a*) shows that in the range of $Y_{fa} = 0.0$ to $Y_{fa} = 1.736741$ (corresponding to a SLP), a multiplicity of steady states exists. Three possible static solutions are present in this range: two solutions give stable branches (solid lines) and one solution gives the unstable branch (dashed line). The low temperature stable branch is physically unrealistic for the reactor dense phase temperature is lower than the vaporization temperature of gasoil ($Y_v = 1.078$). Both stable branches give very low gasoline yields as seen from Figure 2(*b*). The highest gasoline yield ($X_{gd} = 0.438505$) occurs at the middle unstable branch. $Y_{RD} = 1.24234$ and $Y_{fa} = 1.313738$ correspond to maximum gasoline yield. For values of air feed temperatures higher than $Y_{fa} = 1.736741$, the high temperature stable steady states branch exists as a unique, globally stable branch with low gasoline yield (Figure 2(*b*)).

3.1.2. Second Region, R2 (0.7653 < F_{CDS} < 1.502964)

This is the region which extends from $F_{CDS} = 0.7653$ (corresponding to homoclinic termination of loci of Hopf bifurcation points with the loci of the static limit point) to $F_{CDS} = 1.502964$. In this region three static limit points and one Hopf bifurcation point (the degenerate HBP is not shown in the figure) exist. The open-loop bifurcation diagram for $F_{CDS} = 1.2$ is shown in Figure 2(*c*), (*d*) for Y_{RD} and X_{gd} respectively against Y_{fa}. Figure 2(*c*) shows that in the range of $Y_{fa} = 0.0$ to $Y_{fa} = 1.384218$ (corresponding to a SLP) multiplicity of steady states exists. Three possible static solutions are present in this range; two solutions give stable branches and one solution gives unstable branch. The low temperature stable branch is still physically unrealistic. Both stable branches give very low gasoline yield as seen from Figure 2(*d*). The highest gasoline yield ($X_{gd} = 0.438715$) occurs at the middle unstable branch. The dense phase reactor temperature which corresponds to maximum gasoline yield is 1.235132 and the dimensionless air feed temperature is 1.374334. A small region [$Y_{fa} = 1.384218$ to $Y_{fa} = 1.387164$ (corresponding to a SLP)] of 5 steady states solutions exists. Two branches are stable and the other remaining three branches are unstable. The stable branches give low gasoline yields as seen from Figure 2(*d*). In the region of $Y_{fa} = 1.387164$ to $Y_{fa} = 1.660117$ (corresponding to a SLP) the number of possible steady solutions reduces from five to three; two of which are stable and the third unstable. Note the Hopf bifurcation point occurs at $Y_{fa} = 1.656844$ which is very close to the static limit point at $Y_{fa} = 1.660117$. For values of $Y_{fa} > 1.660117$ only the high temperature branch exists as a possible stable solution. The gasoline yield obtained with this branch is low as seen from Figure 2(*d*).

3.1.3. Third Region, R3 (0.5077 < F_{CDS} < 0.7653)

This is the region which extends from $F_{CDS} = 0.5077$ (corresponding to $Y_{fa} = 0.0$) to $F_{CDS} = 0.7653$. This region contains three static limit points and two Hopf bifurcation points (the degenerate HBP is not shown in the figure). The open-loop bifurcation diagram for $F_{CDS} = 0.75$ is shown in Figure 2(*e*), (*f*) for the reactor dense phase temperature and dense phase gasoline yield respectively against the dimensionless air feed temperature. Figure 2(*e*) shows that in the range of $Y_{fa} = 0.0$ to $Y_{fa} = 1.336676$ (corresponding to a SLP) three possible static solutions exist; two solutions give stable branches and one solution gives unstable branch. The low temperature stable branch is still physically unrealistic. Both stable branches give very low gasoline yield as seen from Figure 2(*f*). In the region from $Y_{fa} = 1.336676$ to $Y_{fa} = 1.483577$ (corresponding to a HBP) there are 5 steady states branches. Two branches are stable and three unstable. The stable branches give low gasoline yields as seen from Figure 2(*f*). In the small region from $Y_{fa} = 1.483577$ to $Y_{fa} = 1.49205$ (corresponding to a SLP) three stable static branches coexist with two unstable branches. The highest gasoline yield ($X_{gd} = 0.438709$) occurs at the middle stable branch for $Y_{RD} = 1.228803$ and $Y_{fa} = 1.49205$. In the region of $Y_{fa} = 1.49205$ to $Y_{fa} = 1.539331$ (corresponding to a SLP) three steady states branches exist; two branches are stable and the third branch is unstable. Note the Hopf bifurcation point occurs at $Y_{fa} = 1.536299$ which is very close to the static limit point at $Y_{fa} = 1.539331$. At higher values of air feed temperatures ($Y_{fa} > 1.539331$) only the high temperature branch exists as a possible stable solution with low gasoline yield as seen from Figure 2(*f*).

3.1.4. Fourth Region, R4 (0.202217 < F_{CDS} < 0.5077)

This is the region which extends from F_{CDS} = 0.202217 (corresponding to the lower turning point of the loci of limit points) to F_{CDS} = 0.5077. This region contains four static limit points and two Hopf bifurcation points (the degenerate HBP not shown in the figure). The open-loop bifurcation diagram for F_{CDS} = 0.4 is shown in Figure 2(*g*) for Y_{RD} and Figure 2(*h*) for X_{dg} against the dimensionless air feed temperature. Figure 2(*g*) shows that in the range of Y_{fa} = 0.0 to Y_{fa} = 0.617242 (corresponding to a SLP on the upper branch) a unique, globally stable low temperature branch exists. The gasoline yield obtained with this branch is extremely low (almost zero) as seen from Figure 2(*h*). From Y_{fa} = 0.617242 to Y_{fa} = 1.244646 (corresponding to a SLP) three possible static solutions exist; two are stable and one unstable. Both stable branches give very low gasoline yield as seen from Figure 2(*h*). The region from Y_{fa} = 1.244646 to Y_{fa} = 1.363358 (corresponding to a SLP) contains 5 steady states solutions. Two branches are stable and the other remaining three branches are unstable. The stable branches give low gasoline yields as seen from Figure 2(*h*). Note that this region contains a degenerate Hopf bifurcation point at Y_{fa} = 1.36090. The region from Y_{fa} = 1.363358 to Y_{fa} = 1.551989 (corresponding to a HBP) a stable periodic solution emanating from the Hopf bifurcation point at Y_{fa} = 1.551989 coexists with a stable static solution and unstable static branch. The region from Y_{fa} = 1.551989 to Y_{fa} = 1.815091 (corresponding to a SLP) shows the coexistence of two stable branches with one unstable branch. The temperature of the lower stable branch is higher than the vaporization temperature of gasoil. This branch gives the highest stable gasoline yield (X_{gd} = 0.438123) as seen from Figure 2(*h*). The dense phase reactor temperature which corresponds to maximum gasoline yield is 1.226144 and dimensionless air feed temperature is 1.761573. It is clear that obtaining the highest gasoline in a stable fashion requires significantly higher values of air feed temperatures. For Y_{fa} > 1.815091 only the high temperature branch exists as a possible stable solution with low gasoline yield as seen from Figure 2(*h*).

3.1.5. Fifth Region, R5 (0.0 < F_{CDS} < 0.202217)

This is the region which extends from F_{CDS} = 0.0 to F_{CDS} = 0.202217. In this region two static limit points and two Hopf bifurcation points (the degenerate HB point is not shown in the figure) exist. The open-loop bifurcation diagrams for F_{CDS} = 0.2 are shown in Figure 2(*i*) for Y_{RD} and Figure 2(*j*) for X_{gd} against the dimensionless air feed temperature. Figure 2(*i*) shows that in the range of Y_{fa} = 0.0 to Y_{fa} = 1.1089 (corresponding to a SLP) a unique, globally stable low temperature branch exists. The gasoline yield obtained with this branch is extremely low (almost zero) as seen from Figure 2(*j*). From Y_{fa} = 1.1089 to Y_{fa} = 1.186731 (corresponding to a SLP) three possible static solutions exist: one gives stable steady states and two give unstable steady states. The stable branch gives a very low gasoline yield, as seen from Figure 2(*j*). Note that in this region (Y_{fa} = 1.1089 to Y_{fa} = 1.186731) there is a degenerate Hopf bifurcation point at Y_{fa} = 1.18520. The region from Y_{fa} = 1.1186731 to Y_{fa} = 1.489845 (corresponding to a HBP) contains the stable periodic branch as a unique solution. The whole region (Y_{fa} = 0.0 to Y_{fa} = 1.489845) is physically unrealistic. At values of Y_{fa} > 1.489845 the stable static branch exists as the unique globally stable branch. The maximum gasoline yield is obtained in a stable fashion for Y_{fa} = 2.327567.

Table 2 shows a summary of the qualitative differences (*i.e.* the number of HBPs and SLPs) between the five regions. It is clear from the previous discussion of the various regions that maximum gasoline yield can be obtained in either a stable or unstable fashion depending on the region (*i.e.* operating conditions). The maximum gasoline yield for regions R1 and R2 is unstable whereas it is stable for regions R3, R4, and R5. Figure 3 shows the effect of

Table 2. Qualitative Differences Between Various Regions.

Region	# of SLP	# of HBP
R1	1	1
R2	3	1
R3	3	2
R4	4	2
R5	2	2

catalyst circulation ratio (F_{CDS}) on the optimum air feed temperature (Y_{faopt}). The optimum air feed temperature is the temperature at which air must be fed to the regenerator in order to obtain maximum gasoline yield. It is clear from the figure that Y_{faopt} increases upon decreasing F_{CDS}. The dashed vertical line in figure separates regions that give highest gasoline yield in a stable fashion from unstable ones. The required air feed temperatures in the stable region are higher than their unstable counterparts. Therefore, to operate the fluid catalytic cracking unit at its maximum gasoline yields under reasonable air feed temperatures it is necessary to stabilize the unit. For this purpose a control system must be used.

3.2. Closed-Loop Bifurcation Behavior

A simple feedback proportional controller is used to stabilize and control the unit at the point of maximum gasoline yield. The bifurcation behavior of a controlled unit (closed loop system) is therefore investigated. Regions R1 and R2 are investigated because the maximum gasoline yield is obtained on an unstable branch.

3.2.1. Region 1 (R1)

From the open loop analysis, for $F_{CDS} = 1.7$ the maximum gasoline yield is 0.438505 ($Y_{RD} = 1.24234$ and $Y_{fa} = 1.313738$). The controller gain, Kc, is used as the main bifurcation parameter and the set point of the controller is $Y_{sp} = 1.24234$ and Y_{fa} is the manipulated variable according to Equation (7) ($Y_{fas} = 1.313738$). The bifurcation diagrams for this case are shown in Figure 4(a) for reactor dense phase temperature and Figure 4(b) for gasoline yield against the controller gain. The following important observations can be drawn from the figure.

1. The region from $Kc = 0.0$ (implies the open loop case) to $Kc = 0.3148508$ (corresponding to a SLP) contains three steady states branches. Two branches are stable (the low temperature branch is physically unrealistic) and the third branch is unstable. The gasoline yield obtained from both stable branches is very low (see Figure 4(b)) and the highest gasoline yield is obtained with the unstable branch. Because the operating conditions are set at the highest gasoline yield, there is no branch that gives gasoline yield higher than this branch.

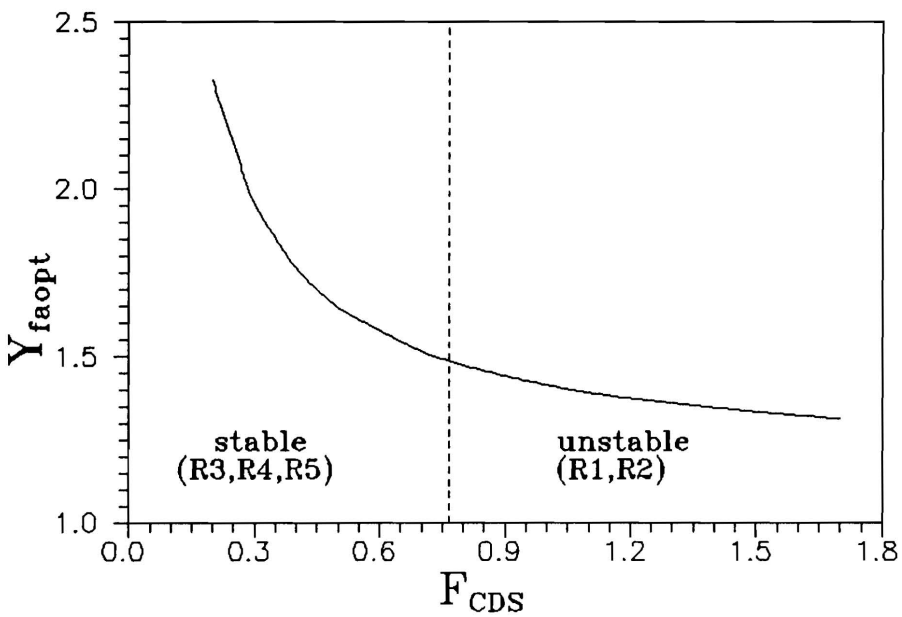

Figure 3. Effect of Catalyst Circulation Ratio, F_{CDS}, on the Optimum Air Feed Temperature, Y_{faopt}. Dashed vertical line separates stable from unstable regions.

2. The region from $Kc = 0.3148508$ to $Kc = 1.484101$ (corresponding to a SLP) contains five steady states branches and a degenerate Hopf bifurcation point at $Kc = 1.464257$. The two stable steady states branches in this region give low gasoline yields as seen from Figure 4(*b*).
3. In the region from $Kc = 1.484101$ to $Kc = 3.594945$ (corresponding to a SLP) only one stable steady states branch coexists with two unstable static branches. The gasoline yield obtained with the stable branch is less than 0.21 as seen from Figure 4(*b*).

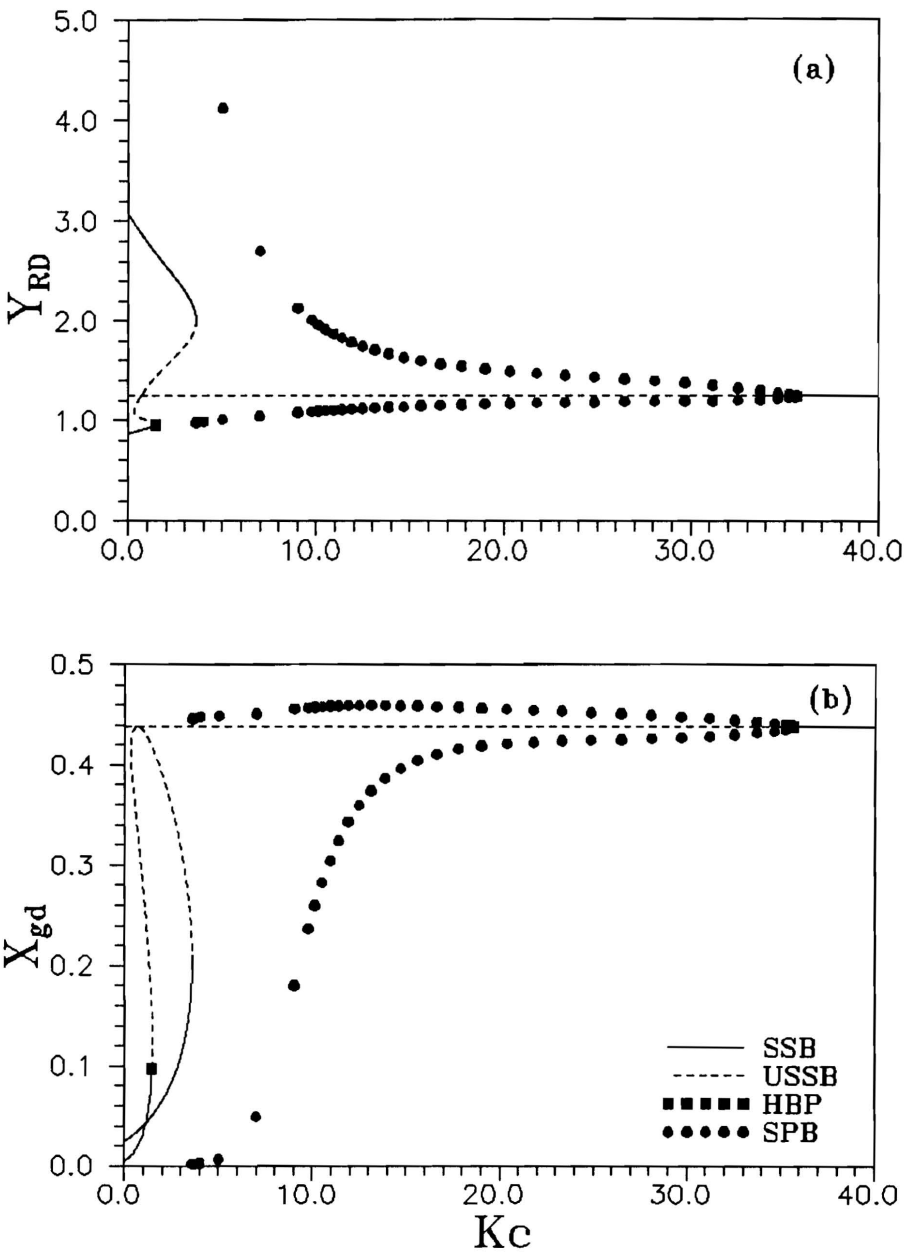

Figure 4. Bifurcation Diagram for Closed Loop System for Catalyst Circulation Ratio, $F_{CDS} = 1.7$ *(Set Point Temperature,* $Y_{sp} = 1.24234$*).* (a) *Reactor dense phase temperature,* Y_{RD}, vs *controller gain,* Kc *and* (b) *gasoline yield,* X_{gd} vs *controller gain,* Kc.

4. The region from $Kc = 3.594945$ to $Kc = 35.640904$ (corresponding to a HBP) contains the periodic branch emanating from the HBP as the unique, globally stable branch. As the value of Kc is decreased from 35.640904 the oscillations of the periodic branch tend to change from soft (simple) oscillations to hard (bursting) oscillations as seen from the simulation results presented in Figure 5(*a*) for $Kc = 30$ and Figure 5(*b*) for $Kc = 4$. Noticeable from Figure 5(*b*) is that during oscillations the reactor dense phase temperature reaches a prohibitively high value ($Y_{RD} > 5.8$) and goes down to temperatures below the vaporization temperature of gasoil (Y_{RD} about 0.98). Also it is clear from the figure that the period of oscillations increases significantly as Kc is decreased (period = 79 s for $Kc = 30$; period = 2749 s for $Kc = 4$).
5. For $Kc > 35.640904$ the unstable steady state which was the purpose of installing the controller becomes stable for the first time. This stable static branch is unique and therefore globally stable.

From above it becomes clear that in order to operate the unit at its maximum gasoline yield impractically high values of controller gains are required.

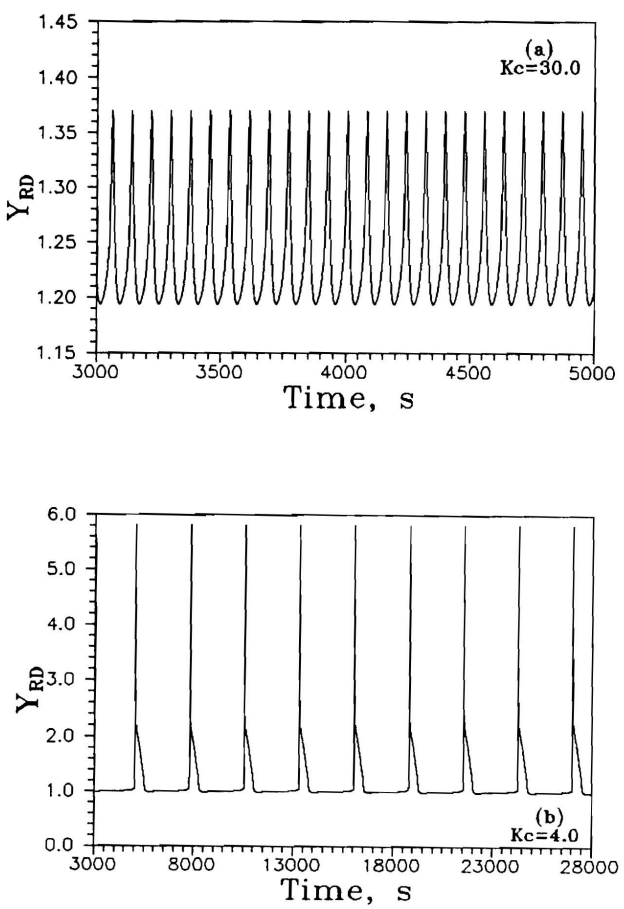

Figure 5. Dynamic Simulation for Reactor Dense Phase Temperature, Y_{RD}, Against Time for (a) *Controller Gain,* Kc = *30 Soft Oscillations and* (b) *Controller Gain,* Kc = *4.0 Hard Oscillations.*

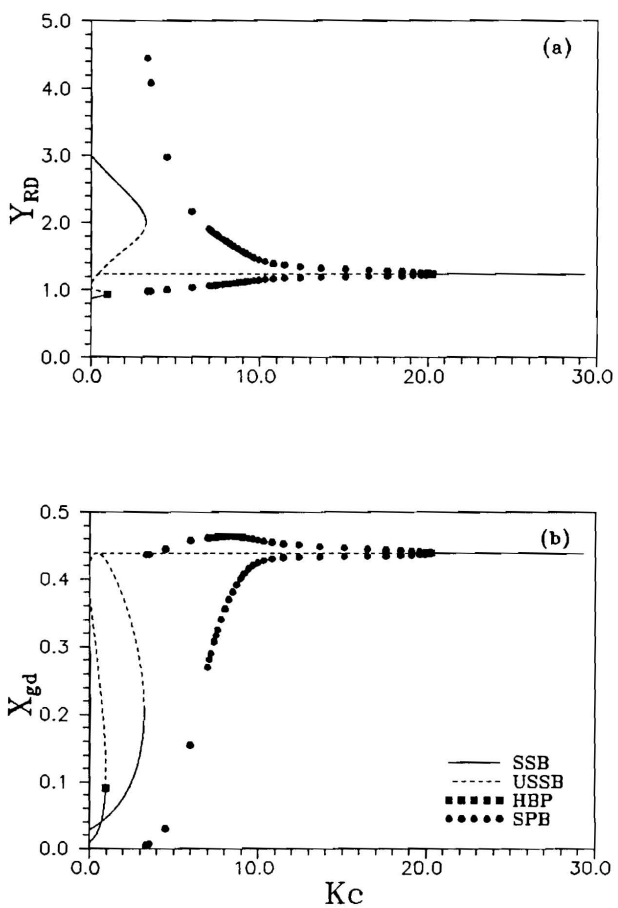

Figure 6. Bifurcation Diagram for Closed Loop System for Catalyst Circulation Ratio, $F_{CDS} = 1.2$ (Set Point Temperature, $Y_{sp} = 1.235132$). (a) *Reactor dense phase temperature, Y_{RD}* vs *controller gain,* Kc *and* (b) *gasoline yield, X_{gd}* vs *controller gain,* Kc.

3.2.2. Region 2 (R2)

At $F_{CDS} = 1.2$, the open loop analysis revealed that the maximum gasoline yield is 0.438715 ($Y_{RD} = 1.235132$ and $Y_{fa} = 1.374334$). The bifurcation diagrams for this case are shown in Figure 6(*a*) for reactor dense phase temperature and Figure 6(*b*) for gasoline yield against the controller gain. Similarly, the following observations can be drawn from the figure.

1. The region from $Kc = 0.0$ (implies the open loop case) to $Kc = 0.00018$ (corresponding to a SLP) contains three steady states branches; two stable branches and one unstable. The gasoline yield obtained from both stable branches is very low (see Figure 6(*b*)) and the highest gasoline yield is obtained with the unstable branch.
2. The region from $Kc = 0.00018$ to $Kc = 0.972121$ (corresponding to a SLP) contains five steady states branches and a degenerate Hopf bifurcation point at $Kc = 0.956714$. The two stable steady states branches in this region give low gasoline yields as seen from Figure 6(*b*).
3. In the region from $Kc = 0.972121$ to $Kc = 3.252644$ (corresponding to a SLP) the stable high temperature steady states branch coexists with two unstable static branches.
4. The region from $Kc = 3.252644$ to $Kc = 20.28624$ (corresponding to a HBP) contains the periodic branch emanating from the Hopf bifurcation point as the unique, globally stable branch. As the value of Kc is decreased from 20.28624 the oscillations of the periodic branch tend to change from soft (simple) oscillations to hard (bursting) oscillations similar to the case above.
5. For $Kc > 20.28624$ there is a unique, globally stable branch which gives low gasoline yield as seen from Figure 6(*b*).

Comparing this case with the former case it is clear that decreasing the catalyst circulation rate tends to decrease the value of the controller gain required to stabilize the system.

4. CONCLUSIONS

The effect of the catalyst circulation rate on the performance of an industrial fluid catalytic cracking unit is investigated for both the open loop and closed loop systems. The investigation covers a wide range of catalyst circulation rate (17.721 to 150.63 kg/s). The two parameter continuation diagram reveals five regions of qualitatively different bifurcation behavior. The open loop analysis shows that decreasing the catalyst circulation rate leads to stabilization of the branch that gives maximum gasoline yield. However, the feed temperature of the air used to burn-off the coke must be dramatically increased as catalyst circulation rate is decreased. The closed loop analysis reveals regions of multiplicity of steady states, globally stable static attractors and globally stable periodic attractors. The analysis also reveals that for certain values of controller gains, transition from simple oscillations to bursting oscillations occurs. During bursting the reactor dense phase temperature reaches prohibitively high values and goes down to temperatures well below the vaporization temperature of gasoil. Higher values of controller gains are required to stabilize the system as catalyst circulation rate is increased.

5. NOTATION

A_1, A_2, A_3	dimensionless groups
A_{IG}, A_{IR}	area of bed within clouds for regenerator and reactor, respectively, m^2.
B, BD	modified space velocities for reactor and regenerator, respectively, 1/s.
C_{alf}	concentration of gasoil in input stream, kg/m^3.
Cpl, Cpf	specific heats of liquid and vaporized gas oil, respectively, kJ/kg.
C_{RD}, C_{GD}	dimensionless group connected with the coke balance in the reactor and regenerator respectively.
F_A	air flow rate, kg/s.
Fc	catalyst circulation rate, kg/s.

F_{CDS} catalyst circulation ratio defined by Equation (8).
F_G gas oil flow rate, kg/s.
G_{CR}, G_{CG} bubble flow rate through any horizontal section for reactor and regenerator, respectively, m^3/s.
G_{IR}, G_{IG} interstitial gas flow rate through any horizontal section for reactor and regenerator, respectively, m^3/s.
H_R, H_G height of reactor and regenerator, respectively, m.
HL_R, HL_G normalized heat losses in reactor and regenerator respectively, 1/s.
HRCB normalized rate of heat absorption due to endothermic cracking reactions in the reactor, 1/s.
Hv normalized heat of vaporization for gas oil, 1/s.
Kc controller gain.
RC coke make rate.
X_{go} dimensionless gas oil concentration.
X_{gd} dimensionless gasoline concentration.
Y_{fa} dimensionless air feed temperature.
Y_{GD} dimensionless regenerator dense phase temperature.
Y_{RD} dimensionless reactor dense phase temperature.
Y_{sp} dimensionless set point reactor temperature.
Yv dimensionless gas oil vaporization temperature.
W_R,W_G catalyst retention in reactor and regenerator, respectively, kg.

Greek Symbols

α_1, α_2, α_3 dimensionless pre-exponential factors for the cracking reactions.
β_c exothermicity factor for coke combustion reaction.
ξ_0 dynamic parameter in heat balance equation for reactor
ξ_1 dynamic parameters in heat balance equation for regenerator.
ξ_2 dynamic parameters for catalyst adsorption capacity for gas oil.
ξ_3 dynamic parameters for catalyst adsorption capacity for gasoline.
ξ_4 dynamic parameters in coke balance equation for reactor.
ξ_5 dynamic parameters in coke balance equation for regenerator.
ε bed voidage.
ψ_R catalyst activity within reactor.
ψ_G catalyst activity within regenerator.
ρ_0, ρ_l, ρ_f density of air, liquid gas oil, vaporized gas oil, respectively, kg/m^3.

Abbreviations

CCR catalyst circulation rate, kg/s.
CSO clarified oil, kg/s.
HBP Hopf bifurcation point.
HCO heavy cycle oil, kg/s.
LCO light cycle oil, kg/s.
SLP static limit point.
SPB stable periodic branch.
SSB stable static branch.
USSB unstable static branch.

REFERENCES

[1] L. Iscol, "The Dynamics and Stability of a Fluid Catalytic Cracker", *Proceedings of the Automatic Control Conference, Atlanta, Georgia, U.S.A.*, 1970, pp. 602–607.

[2] S. S. E. H. Elnashaie and I. M. El-Hennawi, "Multiplicity of the Steady States in Fluidized Bed Reactors—IV. Fluid Catalytic Cracking", *Chem. Engng. Sci.*, **34** (1979), pp. 1113–1121.

[3] W. M. Edwards and H. N. Kim, "Multiple Steady States in Fluidized Bed FCC Unit Operation", *Chem. Engng. Sci.*, **37** (1988), pp. 1611–1623.

[4] S. S. Elshishini and S. S. E. H. Elnashaie, "Digital Simulation of Industrial Fluid Catalytic Cracking Units—I. Bifurcation and Its Implications", *Chem. Engng. Sci.*, **45** (1990), pp. 553–559.

[5] J. M. Arandes and H. I. De Lasa, "Simulation and Multiplicity of the Steady States in Fluidized FCCUs", *Chem. Engng. Sci.*, **47** (1992), pp. 2535–2540.

[6] S. S. E. H. Elnashaie and S. S. Elshishini, "Digital Simulation of Industrial Fluid Catalytic Cracking Units—IV. Dynamic Behavior", *Chem. Engng. Sci.*, **48** (1993), pp. 567–583.

[7] S. S. E. H. Elnashaie, A. E. Abasaeed, and S. S. Elshishini, "Digital Simulation of Industrial Fluid Catalytic Cracking Units—V. Static and Dynamic Bifurcation Behavior", *Chem. Engng. Sci.*, **50** (1995), pp. 1635–1644.

[8] D. Kunii and O. Levenspiel, *Fluidization Engineering*. New York: John Wiley & Sons, 1969.

[9] V. W. Weekman and D. M. Nace, "Kinetics of Catalytic Cracking Selectivity in Fixed, Moving and Fluid Bed Reactors", *A. I. Ch. E. J.*, **16** (1970), pp. 397–404.

[10] E. J. Doedel and J. P. Kernevez, *Auto: Software for Continuation and Bifurcation Problems in Ordinary Differential Equations*. Pasedena, California, U. S. A.: California Institute of Technology, 1986.

Paper Received 24 June 1995; Revised 17 December 1995; Accepted 8 January 1996.